

OPEN ACCESS

Determination of Transport Properties of Electrolyte With or Without Convection

To cite this article: C. Delacourt and C. Rabette 2023 *J. Electrochem. Soc.* **170** 043502

View the [article online](#) for updates and enhancements.

You may also like

- [\(Invited\) Thermodynamics, Stress, and Stefan-Maxwell Diffusion in Solids: Application to Small-Strain Materials Used in Commercial Lithium-Ion Batteries](#)
Daniel R Baker, Mark W Verbrugge and Allan F Bower
- [A Model for Mass Transport of Molten Alkali Carbonate Mixtures Applied to the MCFC](#)
Andreas Bodén and Göran Lindbergh
- [Negative Stefan-Maxwell Diffusion Coefficients and Complete Electrochemical Transport Characterization of Homopolymer and Block Copolymer Electrolytes](#)
Irene Villaluenga, Danielle M. Pesko, Ksenia Timachova et al.



Your Lab in a Box!

The PAT-Tester-i-16: All you need for Battery Material Testing.

- ✓ All-in-One Solution with integrated Temperature Chamber!
- ✓ Cableless Connection for Battery Test Cells!
- ✓ Fully featured Multichannel Potentiostat / Galvanostat / EIS!

www.el-cell.com +49 40 79012-734 sales@el-cell.com

EL-CELL[®]
electrochemical test equipment





Determination of Transport Properties of Electrolyte With or Without Convection

C. Delacourt[✉] and C. Rabette[✉]

Laboratoire de Réactivité et Chimie des Solides, UMR CNRS 7314, Université de Picardie Jules Verne, 80039 Amiens cedex, France

There is a variety of electrochemical methods to determine the transport properties of electrolytes. There are also different underlying hypotheses to derive transport equations that are used in these methods. In this work, we examine how the values of the transport properties determined with some of these methods are affected depending on whether convection is neglected in the Onsager-Stefan-Maxwell transport equations. In particular, we show that the values of the diffusion coefficient and the cation transference number that are determined from analyses of experimental data that ignore convection deviate from those that account for it. We exemplify our point using simulations. This work emphasizes that transport properties from the literature can be used in a mathematical model providing the underlying assumptions of the model are compatible with those used for their determination. © 2023 The Author(s). Published on behalf of The Electrochemical Society by IOP Publishing Limited. This is an open access article distributed under the terms of the Creative Commons Attribution 4.0 License (CC BY, <http://creativecommons.org/licenses/by/4.0/>), which permits unrestricted reuse of the work in any medium, provided the original work is properly cited. [DOI: 10.1149/1945-7111/acc614]



Manuscript submitted August 30, 2022; revised manuscript received February 13, 2023. Published April 17, 2023.

List of Symbols

A	Cell area, m ²
A_1	Coefficient in Eq. 37, mol/m ³
c	Salt concentration, mol/m ³
c_{bottom}	Salt concentration adjacent to the bottom electrode, mol/m ³
c_i	Concentration of species i , mol/m ³
c_T	Sum of species concentrations, mol/m ³
c_{top}	Salt concentration adjacent to the top electrode, mol/m ³
c_∞	Initial salt concentration, mol/m ³
D	Fickian salt diffusion coefficient in the molal scale, m ² /s
D'	Fickian salt diffusion coefficient in the molar scale, m ² /s
\bar{D}	Thermodynamic salt diffusion coefficient, m ² /s
F	Faraday's constant, 96,487 C mol ⁻¹
$\bar{\gamma}_\pm$	Mean molar activity coefficient of the salt
\vec{i}	Ionic current density, A/m ²
\vec{i}_{ss}	Current density at steady state, A/m ²
i_0	Initial current density, A/m ²
i_{app}	Applied current density, A/m ²
L	Thickness of the electrolyte layer, m
m	Salt molality, mol/kg
M	Salt molar weight, kg/mol
M_i	Molar weight of species i , kg/mol
n	Number of electrons exchanged or number of moles of salt, mol
n_i	Number of moles of species i , mol
N_e	Newman number, as defined in Ref. 18
\vec{N}_i	Flux density of species i , mol/m ² -s
Q	Coefficient, as defined in Ref. 6
R	Ideal gas constant, J/K-mol
s_i	Stoichiometric coefficient of species i in a reaction
T	Temperature, K
t	Time, s
t_i^j	Transference number of species i with respect to species j
$t_i^{j'}$	Transport number of species i with respect to species j
\bar{V}_i	Partial molar volume of species i , m ³ /mol
\vec{v}_i	Velocity of species i , m/s
\vec{v}^\square	Volume-averaged velocity of the electrolyte, m/s
\vec{v}_{bottom}	Velocity of the bottom electrode interface, m/s

\vec{v}_{top}	Velocity of the top electrode interface, m/s
z_i	Charge number of species i
Greek	
α	Thermodynamic factor of the electrolyte in the molal scale
α'	Thermodynamic factor of the electrolyte in the molar scale
Φ	Electric potential, V
Φ_{ss}	Electric potential at steady state, V
Φ_0	Electric potential at initial time, V
γ_\pm	Mean molal activity coefficient of the salt
κ	Conductivity, S/m
μ_i	Electrochemical potential of species i , J/mol
ν	Total number of moles of ions into which a mole of salt dissociates
ν_i	Number of moles of ionic species i into which a mole of salt dissociates
ρ	Density, kg/m ³
Subscripts	
e	Parameter that relates to the salt
0	Parameter that relates to the solvent
+	Parameter that relates to the cation
−	Parameter that relates to the anion

In the recent years, physics-based continuum models of batteries have become increasingly popular, both at academic and industrial scale, such that numerous simulation codes emerged (either proprietary or open-source). Among the different physics-based models these codes rely upon,¹ the pseudo-2 dimensional model by Doyle, Fuller, and Newman (DFN) from the mid-90's has been the most popular.²⁻⁴ In this model, the transport of species in the electrolyte is modeled using the concentrated solution theory (Onsager-Stefan-Maxwell -OSM- equations), and the electrolyte is treated as binary (i.e., a mixture of a salt and a single solvent) although battery electrolyte formulation can be somewhat complex (e.g., mixtures of a number of solvents, a salt and/or additives). Flux-explicit equations are derived using the solvent as the reference species in the expressions of the cation and anion flux densities. The solvent velocity is assumed to be zero, regardless of whether an ion-conducting polymer² or a liquid electrolyte^{3,4} is considered. Later on, Dees et al. reported a battery model in which electrolyte transport equations are based on the volume-averaged velocity of the electrolyte.⁵ This model, built upon the seminal work by Newman and Chapman,⁶ was used to simulate impedance spectroscopy. Although Dees et al. would not mention it explicitly, and unlike the DFN battery model, the convection due to the buildup of a

[✉]E-mail: Charles.delacourt@u-picardie.fr

density gradient across electrodes and separator is properly addressed with the set of transport equations they use in their model. Compared to those of the DFN model, these equations require two additional parameters, namely the partial molar volumes of salt \bar{V}_e and solvent \bar{V}_0 of the electrolyte. Nyman et al. used a slightly different approach to analyze the relaxation potential of a Li-Li symmetric cell and arrived at electrolyte transport equations equivalent to those of Dees et al.⁷ Liu and Monroe published a comprehensive work, shedding light on the effects of volume redistribution induced by density gradients (denoted as excluded-volume effects) and faradaic convection due to the moving electrode/electrolyte boundaries during electrochemical reactions at the interfaces.^{8,9} They conclude from this study that both of these effects are relevant when modeling nonaqueous electrolytes such as those used in Li-ion batteries.

When modeling experimental battery data, it is common practice to rely on electrolyte properties from the literature or from online databases.^{10,11} This raises the question of whether the intended application is compatible with the model formulation used to determine the selected model parameters. This issue is extensively discussed in the literature when it comes to the differences between parameters determined using the concentrated or dilute solution theories.¹² There has also been some works comparing parameter values used in OSM and (Poisson-)Nernst-Planck theoretical frameworks.^{13,14} In this work, we rather focus on the influence of accounting for density-gradient-driven convection phenomena on the determination of the transport properties, within the OSM theory framework, building upon the detailed theoretical work by Liu and Monroe.^{8,9} The importance of accounting for convection due to local changes in density has been recently re-stated in a recent review on physics-based model parametrization, because it may skew the values of salt diffusion coefficient and cation transference numbers.¹¹ In the present work, we carefully examine two analytical methods that allow the determination of the salt diffusion coefficient and the cation transference number, namely the restricted diffusion method^{6,15–17} and the steady-state polarization method,^{12,18} respectively. Through a careful derivation of the transport equations, we demonstrate that the restricted diffusion method provides us with different diffusion coefficients, the nature of which depends on the underlying model assumptions. On the contrary, the steady-state polarization method is invariant with the underlying assumption of ignoring convection or not. Nevertheless, a spurious transference number is obtained if the input diffusion coefficient is misleadingly selected *a priori*. These theoretical results are illustrated by applying these two methods to simulations used as surrogate data.

Transport Equations for the Concentrated Binary Electrolyte

A binary electrolyte is considered here, wherein a multivalent salt $(M^{z+})_{\nu_+}(X^{z-})_{\nu_-}$ dissolves into a solvent “0”. The flux densities of the cation and the anion are expressed as (Eqs. 12.8 and 12.9 of Ref. 19)

$$\vec{N}_+ = c_+ \vec{v}_+ = -\frac{\nu_+ D}{\nu RT} \frac{c_T}{c_0} c \nabla \mu_e + \frac{\vec{i} t_+^0}{z_+ F} + \nu_+ c \vec{v}_0, \quad [1]$$

$$\vec{N}_- = c_- \vec{v}_- = -\frac{\nu_- D}{\nu RT} \frac{c_T}{c_0} c \nabla \mu_e + \frac{\vec{i} t_-^0}{z_- F} + \nu_- c \vec{v}_0, \quad [2]$$

where the solvent velocity is used as the reference. Notations are similar to those in Ref. 19 and are listed in the list of symbols.

If another reference velocity is used, then the flux density expressions would need reworking. For instance, if the volume-average velocity is used (Eq. 13 from Ref. 6), then flux densities read:

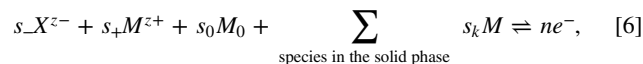
$$\vec{N}_+ = c_+ \vec{v}_+ = -\frac{\nu_+ D c_T \bar{V}_0}{\nu RT} c \nabla \mu_e + \frac{\vec{i} t_+^0}{z_+ F} + \nu_+ c \vec{v}^\square, \quad [3]$$

$$\vec{N}_- = c_- \vec{v}_- = -\frac{\nu_- D c_T \bar{V}_0}{\nu RT} c \nabla \mu_e + \frac{\vec{i} t_-^0}{z_- F} + \nu_- c \vec{v}^\square, \quad [4]$$

in which \vec{v}^\square from original equations in Ref. 6 is conveniently set to zero, and the volume-average velocity is defined as⁶

$$\vec{v}^\square = c_0 \bar{V}_0 \vec{v}_0 + c \bar{V}_e (t_-^0 \vec{v}_+ + t_+^0 \vec{v}_-). \quad [5]$$

The electric potential is introduced by means of an arbitrary electrochemical reaction that is defined as



in which neutral species in the solid phase of the electrode may be involved. The ionic current density is expressed by using the MacInnes equation (Eq. 12.27 of Ref. 19)

$$\vec{i} = -\kappa \nabla \Phi - \frac{\kappa}{F} \left(\frac{s_+}{\nu \nu_+} + \frac{t_+^0}{z_+ \nu_+} - \frac{s_0 c}{n c_0} \right) \nabla \mu_e. \quad [7]$$

At this stage, it is convenient to introduce a so-called Fickian salt diffusion coefficient D that relates to a salt concentration gradient ∇c in the flux expressions (Eqs. 3 and 4) instead of the thermodynamic diffusion coefficient \mathcal{D} that relates to a gradient of the salt chemical potential $\nabla \mu_e$. This is done following Eq. 12.13 of Ref. 19

$$\frac{D c_T \bar{V}_0}{\nu RT} c \nabla \mu_e = D \nabla c. \quad [8]$$

From a thermodynamic derivation of $\nabla \mu_e = \nu RT \left(1 + \frac{d \ln f_{\pm}}{d \ln c} \right) \frac{\nabla c}{c} = \nu RT \left(1 + \frac{d \ln \gamma_{\pm}}{d \ln m} \right) \frac{1}{c_0 \bar{V}_0} \frac{\nabla c}{c}$, the Fickian diffusion coefficient is expressed as (Eq. 12.12 of Ref. 19)

$$D = \mathcal{D} \frac{c_T}{c_0} \left(1 + \frac{d \ln \gamma_{\pm}}{d \ln m} \right) = \mathcal{D} c_T \bar{V}_0 \left(1 + \frac{d \ln f_{\pm}}{d \ln c} \right), \quad [9]$$

which we denote as the *diffusion coefficient in the molal scale* in this work.

The symmetric cell.—Let us consider a symmetric cell that relies on the above arbitrary reaction 6 at both electrodes. In this cell, the electrodes are considered planar, so that the problem is treated along a single dimension (1D) across the cell. The reaction occurs cathodically at one electrode and anodically at the other, so that the electrolyte composition remains unchanged in average. Although the problem is 1D, for the sake of simplicity in notations, we keep them general in the following, except for the boundary conditions. To model the cell operation, the set of governing equations includes a mass balance on, e.g., the anion of the salt

$$\nu_- \frac{\partial c}{\partial t} = -\nabla \cdot \vec{N}_-, \quad [10]$$

the MacInnes Eq. 7, an equation of state

$$c_0 \bar{V}_0 + c \bar{V}_e = 1, \quad [11]$$

a mass balance on the solvent

$$\frac{\partial c_0}{\partial t} = -\nabla \cdot \vec{N}_0 = -\nabla \cdot (c_0 \vec{v}_0), \quad [12]$$

and a current balance

$$\nabla \cdot \vec{i} = 0. \quad [13]$$

After the anion flux is replaced by its expression 2 in mass balance 10, and the current density is replaced by its expression 7 in current balance 13, the remaining variables to solve for are the electric potential, the salt and solvent concentrations, and the solvent velocity.

The cell is such that the bottom electrode is immobile, whereas the top electrode is mobile (Fig. 1).

The boundary conditions are such that Faraday equations for, e. g., anion, apply at the boundary between the immobile electrode and the electrolyte

$$\vec{N}_- - \nu_- c \vec{v}_{bottom} = -\frac{s_-}{nF} \vec{i} \quad [14]$$

Another boundary condition specifies the solvent velocity

$$\vec{N}_0 - c_0 \vec{v}_{bottom} = c_0 (\vec{v}_0 - \vec{v}_{bottom}) = -\frac{s_0}{nF} \vec{i} \quad [15]$$

In the above two equations, \vec{v}_{bottom} denotes the velocity of the boundary of the immobile electrode, which is due to the deposition/stripping of solid species, and it relates to the current density according to⁸

$$\vec{v}_{bottom} = -\frac{\sum_{\text{species in the solid phase}} s_k \vec{V}_k}{nF} \vec{i} \quad [16]$$

At the mobile electrode, the velocity of the boundary is such that

$$\vec{v}_{top} = \vec{v}_{bottom} + \frac{dL}{dt} \vec{e}_x, \quad [17]$$

with L the thickness of the electrolyte layer that is expressed as

$$L = \frac{1}{A} \int \vec{V}_e dn + \frac{1}{A} \int \vec{V}_0 dn_0, \quad [18]$$

where A is the cross-section area of the cell that is taken as a constant, i.e. any volume change of the electrolyte results into a change of the interelectrode thickness. It is customary to assume that partial molar volumes of solvent and salt are not composition dependent. With this assumption, the electrolyte density varies linearly with the salt concentration according to

$$\rho = \left(M - \frac{M_0 \bar{V}_e}{\bar{V}_0} \right) c + \frac{M_0}{\bar{V}_0}, \quad [19]$$

in agreement with experimental data for a number of electrolytes (e. g., in Ref. 20). With constant partial molar volumes, it results from Eq. 18 that the electrolyte thickness L is invariant, and from Eq. 17, it results that boundaries of immobile and mobile electrodes move at the same velocity \vec{v}_{bottom} . Under these conditions, the solution of the problem is not affected by the moving boundaries, as discussed by Liu and Monroe.⁸ Therefore, the movement of the boundary due to the possible formation/consumption of solid products/reactants at the electrode surface is ignored in the following, or in other words, positions and velocities are defined in a referential that is immobile with respect to the boundaries for simplicity. Hence, boundary conditions 14 and 15 simplify to

$$\vec{N}_- = -\frac{s_-}{nF} \vec{i}, \quad [20]$$

and

$$\vec{N}_0 = -\frac{s_0}{nF} \vec{i}, \quad [21]$$

respectively. Finally, a boundary condition requires that the potential is set to zero at a boundary (reference point for potential). and

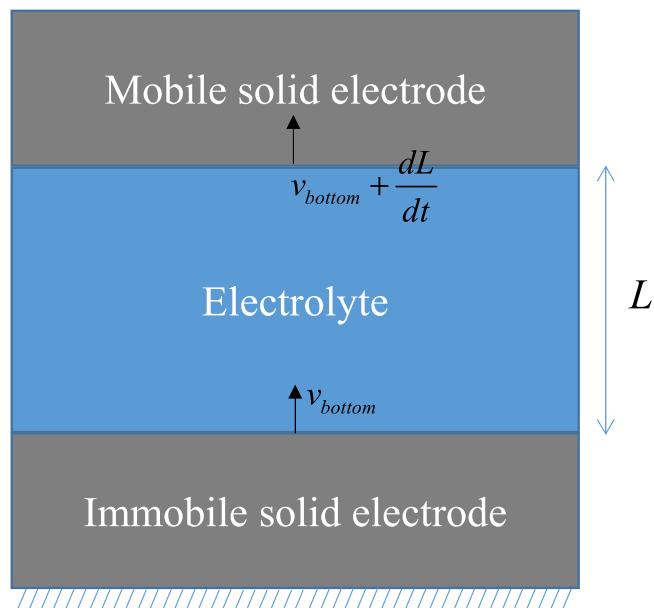


Figure 1. Schematics of the symmetric cell.

another condition either specifies the current density or the electric potential of the electrolyte at the other boundary.

Now, if using the framework based on volume-average velocity, the mass balance Eq. 10 on anion reads

$$\frac{\partial c}{\partial t} = -\nabla \cdot \left(-D \nabla c + \frac{\vec{i} t_-^0}{z_- \nu_- F} + c \vec{v} \square \right), \quad [22]$$

that on cation reads

$$\frac{\partial c}{\partial t} = -\nabla \cdot \left(-D \nabla c + \frac{\vec{i} t_+^0}{z_+ \nu_+ F} + c \vec{v} \square \right), \quad [23]$$

and that on solvent reads

$$\frac{\partial c_0}{\partial t} = -\nabla \cdot (-D \nabla c_0 + c_0 \vec{v} \square) \quad [24]$$

Multiplying Eq. 23 by \vec{V}_e and Eq. 24 by \vec{V}_0 , summing, and using the equation of state Eq. 11 to simplify (reminding that partial molar volumes are assumed constant), it comes

$$\nabla \cdot \left(\vec{V}_e \frac{\vec{i} t_+^0}{z_+ \nu_+ F} + \vec{v} \square \right) = 0, \quad [25]$$

which requires that

$$\vec{v} \square = -\vec{V}_e \frac{\vec{i} t_+^0}{z_+ \nu_+ F} + cst, \quad [26]$$

The integration constant cst is determined from the boundary conditions on $\vec{v} \square$ at the immobile electrode (obtained by using Faraday's equations and Eq. 5 and rearranging)

$$\vec{v} \square = -\frac{\vec{i}}{F} \left[\frac{\bar{V}_0 s_0}{n} + \vec{V}_e \left(\frac{s_+ z_+}{n \nu_+ z_+} + \frac{t_+^0}{\nu_+ z_+} \right) \right] \quad [27]$$

which holds true throughout the cell. The integration constant reads

$$cst = -\frac{\vec{i}}{nF} \left[\bar{V}_0 s_0 + \frac{s_+ \bar{V}_e}{\nu_+} \right]. \quad [28]$$

The mass balance on anion, after the volume-average velocity is replaced by its expression (Eq. 27) becomes

$$\frac{\partial c}{\partial t} = \nabla \cdot \left(D \nabla c + \frac{\vec{i}}{z_+ \nu_+ F} (1 - t_+^0 c_0 \bar{V}_0) + \frac{\vec{i}}{F} \frac{\bar{V}_0 s_0}{n} c + \frac{\vec{i}}{F} c \bar{V}_e \left(\frac{s_+}{n \nu_+} \right) \right), \quad [29]$$

The boundary condition on anion flux (Eq. 20) states that

$$\vec{N}_- = c_- \vec{v}_- = -\nu_- D \nabla c + \frac{\vec{i} t_-^0}{z_- F} + \nu_- c \vec{v} \square = -\frac{s_- \vec{i}}{n F} \quad [30]$$

Substitution of the right hand side term of Eq. 27 for the volume-average velocity in Eq. 30 yields

$$-D \nabla c - \frac{\vec{i}}{F} \left[\frac{\bar{V}_0 s_0}{n} c - \frac{c \bar{V}_e}{z_+ \nu_+} + c \bar{V}_e \frac{(s_-)}{n \nu_-} + c \bar{V}_e \frac{t_+^0}{\nu_+ z_+} - \frac{t_+^0}{z_+ \nu_+} \right] = -\frac{\vec{i}}{n F \nu_+} s_+ \quad [31]$$

It can be shown that an equivalent expression as Eq. 31 is derived if the boundary condition on the cation flux is used instead.

In case reaction (6) is $-M^{z+} + M_{solid} \rightleftharpoons z_+ e^-$ (i.e., $s_0 = s_- = 0$, $s_+ = -1$, and $n = z_+$), mass balance Eq. 29 simplifies to

$$\frac{\partial c}{\partial t} = \nabla \cdot \left(D \nabla c + \frac{\vec{i}}{z_+ \nu_+ F} c_0 \bar{V}_0 (1 - t_+^0) \right) \quad [32]$$

and the boundary condition Eq. 31 becomes

$$-D \nabla c - \frac{\vec{i}}{\nu_+ z_+ F} (1 - c \bar{V}_e) (1 - t_+^0) = -D \nabla c - \frac{\vec{i}}{\nu_+ z_+ F} (c_0 \bar{V}_0) t_-^0 = 0 \quad [33]$$

Transport Equations When Solvent Velocity is Set to Zero

In the literature, the solvent is often taken as the reference species in flux expressions, instead of the convenient derivation using the volume-averaged velocity by Newman and Chapman. In this situation, it is customary to simplify the treatment of transport by assuming v_0 is small enough for the convection term to be zero in Eqs. 1 and 2.²⁻⁴ The symmetric cell problem laid out above is simplified because there is no longer the need to solve for the mass balance on solvent (Eq. 12). After inserting the flux expression (Eq. 2), the mass balance on the anion (Eq. 10), becomes

$$\frac{\partial c}{\partial t} = \nabla \cdot \left(\frac{D}{c_0 \bar{V}_0} \nabla c + \frac{\vec{i} (1 - t_+^0)}{z_+ \nu_+ F} \right) \quad [34]$$

At this stage, notice that Eq. 32 (which is suitable when the electrochemical reaction includes neither the solvent nor the anion) differs from Eq. 34 (that has no condition on either s_0 or s_-). The difference is there as long as $\frac{1}{c_0 \bar{V}_0} = 1 - \frac{d \ln c_0}{d \ln c}$ differs from one. In this work, we introduce a so-called salt diffusion coefficient *in the molar scale* as

$$D' = \frac{D}{c_0 \bar{V}_0} = \mathcal{D} \frac{c_T}{c_0} \left(1 + \frac{d \ln \gamma_{\pm}}{d \ln m} \right) \frac{1}{c_0 \bar{V}_0} = \mathcal{D} \frac{c_T}{c_0} \left(1 + \frac{d \ln f_{\pm}}{d \ln c} \right). \quad [35]$$

Likewise, an anion transference number $t_-^{0'}$ is defined such that

$$t_-^{0'} = t_-^0 c_0 \bar{V}_0 \quad [36]$$

Nyman et al. refer to this anion transference number as a transference number with respect to room.⁷ This has been scrutinized

more recently by Hou and Monroe, who denote it as an *anion transport number* t_- instead of the notation here.²¹

Restricted Diffusion Method to Determine the Diffusion Coefficient

The full problem (with convection included).—Harned and French carried out an analysis of the relaxation of the concentration profile in a cell of length L over time, based on the dilute solution theory.¹⁵ Based on appropriate boundary conditions, similar to what was laid out above, with an additional condition on current density across the cell to be zero, Newman and Chapman demonstrated that (at sufficiently long relaxation time) the time dependence of the concentration difference across the cell Δc is described by the following equation^{6,16}

$$\Delta c = c_{top} - c_{bottom} \approx 2A_1 \exp\left(-\frac{\pi^2 D t}{L^2}\right), \quad [37]$$

with A_1 a coefficient that depends on the initial concentration profile across the cell.¹⁶ A potential difference can be measured between the working terminal electrodes used to form the concentration profile, from which the concentration difference Δc is inferred from the Mac Innes Eq. 7 after the current is set to zero¹⁷

$$\begin{aligned} \nabla \Phi &= -\frac{1}{F} \left(\frac{s_+}{\nu_+} + \frac{t_+^0}{z_+ \nu_+} - \frac{s_0 c}{n c_0} \right) \nabla \mu_e \\ &= -\frac{1}{F} \left(\frac{s_+}{\nu_+} + \frac{t_+^0}{z_+ \nu_+} - \frac{s_0 c}{n c_0} \right) \nu RT \left(1 + \frac{d \ln \gamma_{\pm}}{d \ln m} \right) \frac{1}{c_0 \bar{V}_0} \frac{\nabla c}{c} \end{aligned} \quad [38]$$

At long relaxation time, once electrolyte composition is nearly uniform across the cell (and as a consequence, electrolyte thermodynamic and transport properties), an integration of the potential across the cell reads

$$\Delta \Phi = -\frac{1}{F} \left(\frac{s_+}{\nu_+} + \frac{t_+^0}{z_+ \nu_+} - \frac{s_0 c}{n c_0} \right) \nu RT \left(1 + \frac{d \ln \gamma_{\pm}}{d \ln m} \right) \times \frac{1}{c_0 \bar{V}_0} \frac{A}{c} \exp\left(-\frac{\pi^2 D t}{L^2}\right) \quad [39]$$

A plot of $-\ln \Delta \Phi = f(t)$ at long relaxation time is nearly linear, and has a slope of $\frac{\pi^2 D}{L^2}$. Note that the diffusion coefficient that is derived from the slope relates to the thermodynamic one according to Eq. 9, hence it is in the molal scale.

The simplified problem (with convection ignored).—When using a model in which convection is ignored, mass balance 34 is used instead of mass balance 32, and the concentration difference now reads

$$\Delta c = c_{top} - c_{bottom} \approx 2A_1 \exp\left(-\frac{\pi^2 D' t}{L^2}\right), \quad [40]$$

and a plot of $-\ln \Delta \Phi = f(t)$ at long relaxation time is linear and has a slope of $\frac{\pi^2 D'}{L^2}$, where D' is in the molar scale.

Determination of the Transference Number with the Steady-State Polarization Method

The full problem (with convection included).—From an equilibrium state, a potentiostatic step (or a galvanostatic pulse) is applied until the system is at steady state. The potentiostatic step consists in applying a constant potential bias to the cell whereas the galvanostatic pulse consists in applying a constant current to the cell. Under these conditions, and considering a situation where $s_0 = s_- = 0$, the anion flux

$$N_- = -\frac{\nu_- \mathcal{D} c_T \bar{V}_0}{\nu RT} c \nabla \mu_e - \frac{\nu_- \vec{i} t_-^0}{z_+ \nu_+ F} c_0 \bar{V}_0 \quad [41]$$

is zero across the cell, implying that

$$\frac{\mathcal{D}c_T}{\nu RTc_0}c\nabla\mu_e = -\frac{\vec{i}_{ss}t_-^0}{z_+\nu_+F} \quad [42]$$

From MacInnes Eq. 7, the gradient of chemical potential of the salt is eliminated in Eq. 42 so that

$$\vec{i}_{ss}(1 + N_e) = -\kappa\nabla\Phi_{ss}, \quad [43]$$

where

$$N_e = -\frac{\kappa RT}{F^2} \frac{\nu}{z_+\nu_+} \left(\frac{s_+}{n\nu_+} + \frac{1-t_-^0}{z_+\nu_+} \right) \frac{c_0 t_-^0}{\mathcal{D}c_T c} \quad [44]$$

Note that with $s_+ = -1$, which implies $z_+ = n$, N_e simplifies to

$$N_e = \frac{\kappa RT}{F^2} \frac{\nu}{(z_+\nu_+)^2} (t_-^0)^2 \frac{c_0}{\mathcal{D}c_T c} \quad [45]$$

which is equivalent to the equation in Balsara and Newman.¹⁸ Using Eq. 9, it may be convenient to introduce a Fickian diffusion coefficient in N_e

$$N_e = \frac{\kappa RT}{F^2} \frac{\nu}{(z_+\nu_+)^2} (t_-^0)^2 \frac{\left(1 + \frac{d \ln \gamma_{\pm}}{d \ln m}\right)}{Dc} \quad [46]$$

Just after the potentiostatic step (or the galvanostatic pulse) is applied, MacInnes Eq. 7 boils down to

$$\vec{i}_0 = -\kappa\nabla\Phi_0 \quad [47]$$

If a potentiostatic step is applied, then

$$\frac{i_{ss}}{i_0} = \frac{1}{1 + N_e} \quad [48]$$

If a galvanostatic pulse is applied, then

$$\frac{\Delta\Phi_0}{\Delta\Phi_{ss}} = \frac{1}{1 + N_e} \quad [49]$$

The simplified problem (with convection ignored).—In this situation, the anion flux N_- is given by Eq. 2 after the convection term is taken out. Just like in the case with convection, N_- is zero across the cell, leading to

$$\frac{\mathcal{D}c_T}{\nu RTc_0}c\nabla\mu_e = -\frac{\vec{i}_{ss}t_-^0}{z_+\nu_+F}. \quad [50]$$

However, the assumption of ignoring convection in this method is not necessary because the steady state condition requires that $\vec{v}_0 = 0$, thereby cancelling the convection term anyway. An immediate consequence is that the above equation is identical to that obtained for the full problem, with convection included (Eq. 42). When convection is ignored, the measured diffusion coefficient using the

restricted diffusion method is the salt diffusion in the molar scale and is given by Eq. 35. Therefore, except for Eq. 46, one eventually arrives at the same equations as those laid out above for the case with convection. It follows that

$$N_e = \frac{\kappa RT}{F^2} \frac{\nu}{(z_+\nu_+)^2} (t_-^0)^2 \frac{\left(1 + \frac{d \ln f_{\pm}}{d \ln c}\right)}{D'c}. \quad [51]$$

Balsara and Newman arrive at an expression of N_e that follows Eq. 46, which implies that their analysis of diffusion coefficient and transference number accounts for convection effects.¹⁸ In their analysis, Doyle and Newman expressed N_e using Eq. 51, rather than Eq. 46. Although not clearly laid out by the authors, it implies that they rely on a diffusion coefficient in the molar scale, i.e., determined from a formulation where convection is neglected.¹²

On a final note, in the limit of $c_0 \bar{V}_0 \rightarrow 1$, or in other words when $\frac{d \ln c_0}{d \ln c} \rightarrow 0$, it comes that $1 + \frac{d \ln \gamma_{\pm}}{d \ln m} \approx 1 + \frac{d \ln f_{\pm}}{d \ln c}$ and $D \approx D'$. However, this limit is questionable for concentrated solutions such as battery electrolytes, as further discussed in the next section.

Deviation On Diffusion Coefficient and Transference Number

The relative deviation between the diffusion coefficient in the molal and molar scales is expressed as

$$\frac{\Delta D}{D} = \frac{D' - D}{D} = \frac{1}{c_0 \bar{V}_0} - 1 = \frac{c \bar{V}_e}{1 - c \bar{V}_e} \quad [52]$$

Because the determination of the transference number with the steady-state polarization method relies on that of the diffusion coefficient, the relative deviation of transference number is derived from that of diffusion coefficient

$$\frac{\Delta t_+^0}{t_+^0} = \left| \frac{-(1 - t_+^0)}{2t_+^0} \right| \frac{\Delta D}{D} \quad [53]$$

Examples of calculated deviations between D and D' at $c = 1$ mol/L are reported in Table I for a couple of electrolytes by relying on published datasets. Results indicate that the deviations are not negligible, in particular for electrolytes for which $c \bar{V}_e$ substantially differ from zero. The error on transference number calculated with Eq. 53 (resulting from the use of a diffusion coefficient in the molal scale in Eq. 51 or a diffusion coefficient in the molar scale in Eq. 46 is reported in the same table and has values higher than 10% for all selected electrolytes.

Analysis of Simulations with and Without Convection Using the Restricted Diffusion Method and the Steady-State Polarization Method

In this part, we generate surrogate data from a mathematical model of a Li-Li symmetric cell that undergoes a current pulse of 10 h, followed by a 10 h relaxation. The set of governing equations and corresponding boundary conditions that are used in the model are provided in Table II, which also shows how equations are modified whether convection is accounted for or not. Input parameters are typical of those determined for a 1 M LiPF₆ in ethylene carbonate/

Table I. Relative deviations of diffusion coefficients in molal and molar scales and relative errors on transference numbers determined from the steady-state polarization method.

	\bar{V}_e (10^{-6} m ³ /mol)	t_+^0	$\frac{\Delta D}{D}$ (%)	$\frac{\Delta t_+^0}{t_+^0}$ (%)	References
LiPF ₆ in EC:DEC (1:1 wt.) ($T = 25$ °C)	61.2	0.176	6.5%	15.3%	22
LiPF ₆ in EC:DEC (1:1 wt.) ($T = 25$ °C)	56.8	0.165	6.0%	15.2%	20
LiPF ₆ in PC ($T = 25$ °C)	58.86	0.22	6.3%	11.1%	21
LiTFSI in PEO-5K ($T = 90$ °C)	134.5	0.35	15.5%	12.7%	23

Table II. Set of governing equations and boundary conditions used for the galvanostatic simulation. It is appropriate for a univalent electrolyte ($\nu_+ = \nu_- = z_+ = -z_- = 1$), along with $s_+ = -1$ and $s_- = s_0 = 0$ for the electrochemical reaction (Eq. 6) that is used to define the electric potential.

Li foil/electrolyte boundary	Electrolyte domain	Li foil/electrolyte boundary
$N_- = 0$	$\frac{\partial c}{\partial t} = -\frac{\partial N_-}{\partial x}$	$N_- = 0$
$-\kappa \frac{\partial \Phi}{\partial x} + 2 \frac{RT}{F} \kappa (1 - t_+^0) \alpha' \frac{\partial \ln c}{\partial x} = i_{app}$	$\frac{\partial}{\partial x} \left[-\kappa \frac{\partial \Phi}{\partial x} + 2 \frac{RT}{F} \kappa (1 - t_+^0) \alpha' \frac{\partial \ln c}{\partial x} \right] = 0$	$\Phi = 0$
with $N_- = -D \nabla c - \frac{i_{app}}{F} (1 - c \bar{V}_e) (1 - t_+^0)$ for the case with convection included and $N_- = -D' \nabla c - \frac{i_{app}}{F} (1 - t_+^0) = -\frac{D}{1 - c \bar{V}_e} \nabla c - \frac{i_{app}}{F} (1 - t_+^0)$ for the case with convection ignored.		

diethyl carbonate (1:1 in weight) electrolyte, and are provided in Table III along with literature sources they are selected from. Note that lithium-metal working electrodes are assumed ideally polarizable, i.e., there is no kinetic limitation for charge transfer. Experimentally, a way to get closer to the simulated cell potential may consist in placing lithium reference electrodes (by means of e.g., luggin capillaries) to sense the electrolyte potential just outside of the double layer of each working electrode. The potential measured between the two reference electrodes is free of any polarization at the working electrodes.

Simulations are run with Dumbat program,²⁴ based on a control-volume formulation for the discretization of the set of equations, and Crank-Nicholson method is used to evaluate time derivatives. There are 100 nodes across the electrolyte layer and there is an adaptive time stepping between 0.1 and 500 s.

Simulated cell potential from the model that accounts for convection is represented as a blue line in Fig. 2, whereas that from the model that ignores convection is represented as a red line. Voltage traces in (a) show poorly noticeable differences between the

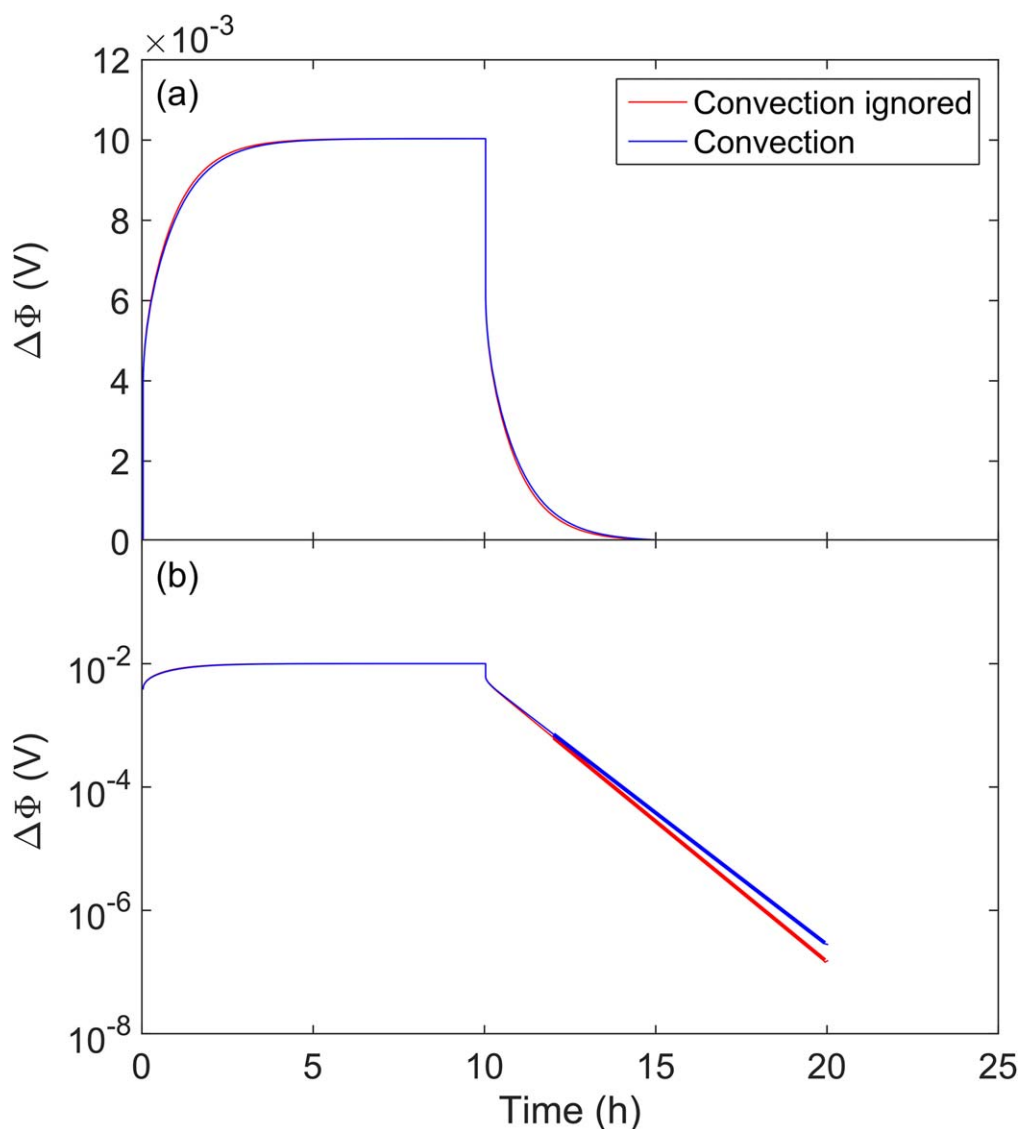


Figure 2. Simulated cell voltage for a Li-Li symmetric cell with parameters typical of a LiPF₆ in EC:DEC (1:1 in weight) electrolyte (Table III), for a 10 h galvanostatic pulse at $i_{app} = 0.1 \text{ mA cm}^{-2}$, followed by an OCV period. Simulation either accounts for convection (blue line) or not (red line). (a) linear plot, (b) semilog plot. Bold lines are linear fits of cell voltage at long relaxation time, used to determine the diffusion coefficient.

Table III. List of model parameters.

Parameter	Symbol	Value	Source
Electrolyte concentration (mol m ⁻³)	c	1,000	set
Solvent concentration (mol m ⁻³)	$c_0 = \frac{1-c\bar{V}_e}{\bar{V}_0}$	10,584	calculated
Thickness of the plain electrolyte layer (m)	L	0.003	set
Partial molar volume of the solvent (m ³ mol ⁻¹)	\bar{V}_0	8.87 10 ⁻⁵	22
Partial molar volume of the salt (m ³ mol ⁻¹)	\bar{V}_e	6.12 10 ⁻⁵	22
Diffusion coefficient (molal scale) (m ² s ⁻¹)	D	2.49 10 ⁻¹⁰	22
Diffusion coefficient (molar scale) (m ² s ⁻¹)	$D' = \frac{D}{c_0\bar{V}_0} = \frac{D}{1-c\bar{V}_e}$	2.65 10 ⁻¹⁰	calculated
Conductivity (S m ⁻¹)	κ	0.789	20
Cation transference number with respect to the solvent	t_+^0	0.183	22
Thermodynamic factor (molal scale)	$\alpha = 1 + \frac{d \ln \gamma_{\pm}}{d \ln c}$	1.548	22
Thermodynamic factor (molar scale)	$\alpha' = 1 + \frac{d \ln f_{\pm}}{d \ln c} = \frac{\alpha}{c_0\bar{V}_0}$	1.649	calculated

Table IV. Values of diffusion coefficient and cation transference number derived from surrogate data (numerical simulations of Fig. 2) using a linear fit of the logarithm of voltage relaxation at long time and the steady-state polarization method, respectively.

	Convection ignored	Convection
Diffusion coefficient from slope of $-\ln \Delta\Phi = f(t)$ in m ² s ⁻¹	$D' = 2.66 \cdot 10^{-10}$	$D = 2.49 \cdot 10^{-10}$
Cation transference number from the steady-state polarization method		
–using Balsara equation (Eq. 46)	0.156	0.183
–using Doyle equation (Eq. 51)	0.183	0.208

two case studies, suggesting that ignoring convection only has a little effect, given the set of input parameters and operating conditions.

In Fig. 2b, a small difference is visible during the cell voltage rise under current and the voltage decrease at medium time of the relaxation, showing a faster dynamics for the case in which convection is ignored. However, as discussed in the theory part of this work, there is no influence of neglecting convection both at initial time and when a steady state is reached during the pulse. Therefore, the transference number determined using the steady-state polarization method is unchanged whether or not convection is neglected.

When representing cell potential in a log scale (Fig. 2b), a marked difference is now visible on the potential decay at long relaxation time. The slope of the linear variation that is seen in the semilog plot is larger in absolute value for the model without convection (red line), which translates to a larger value of the diffusion coefficient derived from the slope, as displayed in Table IV.

An examination of the results in Table IV confirms the theoretical development laid out in the theoretical section:

- D' (diffusion coefficient in the molar scale) is determined from the slope of $-\ln \Delta\Phi = f(t)$ when convection is ignored (Eq. 40). Hence, it is the formulation by Doyle and Newman that is appropriate to derive the cation transference number from the steady-state polarization method (Eq. 51).

- D (diffusion coefficient in the molal scale) is determined from the slope of $-\ln \Delta\Phi = f(t)$ when convection is accounted for (Eq. 37). Using the steady-state polarization method, the proper cation transference number is obtained from the formulation by Balsara and Newman (Eq. 46).

Conclusions

In this work, a careful derivation of Onsager-Stefan-Maxwell transport equations for a concentrated binary electrolyte is carried out, with an emphasis on convection due to electrolyte density gradients. Electrolyte transport equations used in the regular DFN

battery model discards convection phenomena, whereas some other battery modeling works do account for it. When convection is discarded, anion and cation flux-explicit transport equations derived from the OSM theory rely on a so-called diffusion coefficient in the molar scale, denoted as D' herein. On the contrary, when accounting for convection due to density gradients, the OSM flux equations rely on diffusion in the molal scale which is denoted as D . These two diffusion coefficients relate to each other through Eq. 35.

Experimental methods to measure the diffusion coefficient such as the restricted diffusion method, which is quite popular for battery electrolytes, yield a different result depending on whether convection is accounted for or not. Such differences may be substantial; they are in the order of 5% to 15% in the example electrolytes we selected in Table I.

Because the diffusion coefficient is used to derive other transport properties, such as the cation transference number, this transference number itself will vary as well depending on whether convection is accounted for or not. With the steady-state polarization method, differences on yielded values of cation transference numbers amount to 10%–15% for the electrolytes selected as examples in Table I of this work.

As a concluding statement of the above results, it is brought to the reader's attention that model parameters reported in the literature need to be handled carefully. In particular, it must be ensured that an input transport parameter is used in a model that relies on the same hypotheses as those used in the work it is pulled from. It is clearly outlined by the analysis of simulated data from the previous section in order to re-derive diffusion coefficient and cation transference numbers thanks to the restricted diffusion method and the steady-state polarization method, respectively. Along with this conclusion, this work emphasizes the need for tying underlying assumptions to model parameters, in particular when reporting parameters in the form of a database.^{10,11}

Modelers may have to re-compute parameter values so that they are compatible with the model formulation into which these parameters are intended to be used, following the methodology outlined in the previous section.

Acknowledgments

This work is partially founded by the project “Electrolyte Properties for Li-ion Batteries (EP4B)” that is co-funded by the European Union through the “European Regional Development Fund (ERDF)” and the “Région Hauts-de-France.” Authors are grateful to Prof. N. Balsara (University of California, Berkeley) for the initial discussion about this work.

ORCID

C. Delacourt  <https://orcid.org/0000-0001-5241-5441>

C. Rabette  <https://orcid.org/0000-0003-4946-7106>

References

1. F. B. Planella et al., *Prog. Energy*, **4**, 042003 (2022).
2. M. Doyle, T. F. Fuller, and J. Newman, *J. Electrochem. Soc.*, **140**, 1526 (1993).
3. T. F. Fuller, M. Doyle, and J. Newman, *J. Electrochem. Soc.*, **141**, 1 (1994).
4. T. F. Fuller, M. Doyle, and J. Newman, *J. Electrochem. Soc.*, **141**, 982 (1994).
5. D. Dees, E. Gunen, D. Abraham, A. Jansen, and J. Prakash, *J. Electrochem. Soc.*, **152**, A1409 (2005).
6. J. Newman and T. W. Chapman, *AIChE*, **19**, 343 (1973).
7. A. Nyman, M. Behm, and G. Lindbergh, *Electrochim. Acta*, **53**, 6356 (2008).
8. J. Liu and C. W. Monroe, *Electrochim. Acta*, **135**, 447 (2014).
9. J. Liu and C. W. Monroe, *Electrochim. Acta*, **167**, 357 (2015).
10. A. A. Wang et al., *Progress in Energy*, **4**(3), 032004 (2022).
11. A. A. Wang et al., *Prog. Energy*, **4**, 032004 (2022).
12. M. Doyle and J. Newman, *J. Electrochem. Soc.*, **142**, 3465 (1995).
13. M. Lagnoni, C. Nicolella, and A. Bertei, *J. Electrochem. Soc.*, **169**, 020570 (2022).
14. A. M. Bizeray, D. A. Howey, and C. W. Monroe, *J. Electrochem. Soc.*, **63**, E223 (2016).
15. H. S. Harned and D. M. French, *Annals New York Acad. Sci.*, **46**, 267 (1945).
16. S. D. Thompson and J. Newman, *J. Electrochem. Soc.*, **136**, 3362 (1989).
17. Y. Ma, M. Doyle, T. F. Fuller, M. M. Doeff, L. C. D. Jonghe, and J. Newman, *J. Electrochem. Soc.*, **142**, 1859 (1995).
18. N. P. Balsara and J. Newman, *J. Electrochem. Soc.*, **162**, A2720 (2015).
19. J. S. Newman and K. E. Thomas-Alyea, *Electrochemical Systems*. (Wiley Interscience) (2004).
20. H. Lundgren, M. Behm, and G. Lindbergh, *J. Electrochem. Soc.*, **162**, A413 (2015).
21. T. Hou and C. W. Monroe, *Electrochim. Acta*, 135085 (2019).
22. C. Rabette, “Determination of the transport properties of liquid electrolytes for lithium-ion batteries using a multi-electrode electrochemical cell.” *Ph. D. Dissertation*, Université de Picardie Jules Verne (2022).
23. D. M. Pesko, K. Timachova, R. Bhattacharya, M. C. Smith, I. Villaluenga, J. Newman, and N. P. Balsara, *J. Electrochem. Soc.*, **164**, E3569 (2017).
24. C. Delacourt, (2023), <https://charles.delacourt.free.fr/dumbat>.